

# Histological and single-nucleus transcriptome analyses reveal the specialized functions of ligular sclerenchyma cells and key regulators of leaf angle in maize

Qibin Wang<sup>1,3,4</sup>, Qiuyue Guo<sup>2,4</sup>, Qingbiao Shi<sup>1,3</sup>, Hengjia Yang<sup>2</sup>, Meiling Liu<sup>1</sup>, Yani Niu<sup>2</sup>, Shuxuan Quan<sup>2</sup>, Di Xu<sup>1,3</sup>, Xiaofeng Chen<sup>2</sup>, Laiyi Li<sup>2</sup>, Wenchang Xu<sup>1</sup>, Fanying Kong<sup>1</sup>, Haisen Zhang<sup>1</sup>, Pinghua Li<sup>3</sup>, Bosheng Li<sup>2,\*</sup> and Gang Li<sup>1,\*</sup>

<sup>1</sup>State Key Laboratory of Wheat Improvement, College of Life Sciences, Shandong Agricultural University, Tai'an 271018, China

<sup>2</sup>Peking University Institute of Advanced Agricultural Sciences, Shandong Laboratory of Advanced Agriculture Sciences in Weifang, Weifang, Shandong 261325, China

<sup>3</sup>State Key Laboratory of Wheat Improvement, College of Agronomy, Shandong Agricultural University, Tai'an 271018, China

<sup>4</sup>These authors contributed equally to this article.

\*Correspondence: Bosheng Li ([bosheng.li@pku-iaas.edu.cn](mailto:bosheng.li@pku-iaas.edu.cn)), Gang Li ([gangli@sdau.edu.cn](mailto:gangli@sdau.edu.cn))

<https://doi.org/10.1016/j.molp.2024.05.001>

## ABSTRACT

Leaf angle (LA) is a crucial factor that affects planting density and yield in maize. However, the regulatory mechanisms underlying LA formation remain largely unknown. In this study, we performed a comparative histological analysis of the ligular region across various maize inbred lines and revealed that LA is significantly influenced by a two-step regulatory process involving initial cell elongation followed by subsequent lignification in the ligular adaxial sclerenchyma cells (SCs). Subsequently, we performed both bulk and single-nucleus RNA sequencing, generated a comprehensive transcriptomic atlas of the ligular region, and identified numerous genes enriched in the hypodermal cells that may influence their specialization into SCs. Furthermore, we functionally characterized two genes encoding atypical basic-helix-loop-helix (bHLH) transcription factors, bHLH30 and its homolog bHLH155, which are highly expressed in the elongated adaxial cells. Genetic analyses revealed that bHLH30 and bHLH155 positively regulate LA expansion, and molecular experiments demonstrated their ability to activate the transcription of genes involved in cell elongation and lignification of SCs. These findings highlight the specialized functions of ligular adaxial SCs in LA regulation by restricting further extension of ligular cells and enhancing mechanical strength. The transcriptomic atlas of the ligular region at single-nucleus resolution not only deepens our understanding of LA regulation but also enables identification of numerous potential targets for optimizing plant architecture in modern maize breeding.

Wang Q., Guo Q., Shi Q., Yang H., Liu M., Niu Y., Quan S., Xu D., Chen X., Li L., Xu W., Kong F., Zhang H., Li P., Li B., and Li G. (2024). Histological and single-nucleus transcriptome analyses reveal the specialized functions of ligular sclerenchyma cells and key regulators of leaf angle in maize. Mol. Plant. **17**, 920–934.

## INTRODUCTION

Maize (*Zea mays*) is the most extensively cultivated and consumed staple crop worldwide, playing a crucial role in global food security. Over the years, significant yield improvements have been attributed primarily to increased planting densities (Duvick, 2005; Meng et al., 2013; Qin et al., 2016; Assefa et al., 2018; Wang et al., 2020a; Khaipho-Burch et al., 2023). Leaf angle (LA), defined as the inclination angle between the midrib

of the blade and the stem, plays a key role in the regulation of maize plant architecture. A small LA leads to a more upright plant architecture, which mitigates self-shading and minimizes competition from neighboring plants, thereby improving light interception and enhancing photosynthetic productivity at the

---

Published by the Molecular Plant Shanghai Editorial Office in association with Cell Press, an imprint of Elsevier Inc., on behalf of CSPB and CEMPS, CAS.

## Function of sclerenchyma cells in leaf angle regulation

canopy level (Tian et al., 2019; Liu et al., 2021a, 2022; Cao et al., 2022). Although maize hybrid varieties with narrowed LA and compact architecture have been extensively selected in maize production over the past few decades, the complex regulatory mechanisms that govern LA formation remain to be clarified.

In maize, the ligular region serves as a crucial hinge that links the distal blade to the basal sheath, playing a critical role in LA regulation (Mantilla-Perez and Salas Fernandez, 2017). This region is composed of the ligule, a pair of wedge-like auricles, and the central connecting tissue. The ligule, a thin membranous outgrowth at the junction where the blade meets the sheath, acts as a barrier to prevent water, dust, and spores from entering the base of the culm and sheath (Chaffey, 1994, 2008). The auricle, a pair of wedge-like tissues, connects the blade to the sheath, contributing to the erect posture of the plant. Our previous research highlighted the significant role of the auricle, particularly its inner-median region near the midrib (or midvein), in the formation of LA (Kong et al., 2017). Although the physiological functions of the ligule and auricle are well documented, the specific role of the central ligular median (referred to as the LM) remains to be determined. The midrib, auricles, and ligule all converge at this central connecting tissue, forming a nodal-like conserved structure, which highlights its indispensable role in LA regulation.

The development of the ligular region in maize can be categorized into three stages: the early establishment of the blade–sheath boundary, the formation of the preligule band (PLB), and the subsequent development of the ligular region (Cao et al., 2022; Neher et al., 2023). In the initial stage, the demarcation of the ligular region becomes evident as a distinct group of epidermal cells commence division, leading to formation of the PLB, a precursor of the ligule and auricle (Johnston et al., 2014; Neher et al., 2023). The maize *liguleless1* (*lg1*) and *lg2* mutants exhibit defects in the emergence of the ligule and the auricle, resulting in upright leaves and compact plant architecture (Sylvester et al., 1990; Moreno et al., 1997; Walsh et al., 1998), highlighting the critical role of ligular development in the regulation of maize architecture. Following the establishment of the ligular region, variation in cell proliferation and elongation within this area may influence the size of the LA by affecting asymmetric extension on the adaxial or abaxial side of the ligular region.

In recent decades, extensive genetic and molecular studies have revealed that LA is a complex quantitative trait, tightly regulated by numerous internal developmental signals, hormones, and external environmental cues (Kong et al., 2017; Strable et al., 2017; Wang et al., 2022). Among these studies, multiple quantitative trait locus (QTL) analyses and genome-wide association studies have underscored the pivotal roles of *LG1* and *LG2* in LA regulation (Tian et al., 2011; Dzievit et al., 2019; Duan et al., 2022; Zhao et al., 2022). In addition to *LG1* and *LG2*, several other regulators significantly influence the maintenance of ligular regions. These include *BRD1* (Brassinosteroid C-6 oxidase1) and *RAVL1* (Related to *ABI3/VP1-like1*), along with *IL1* (*Increased leaf inclination1*) and *IBH1* (*IL1 binding bHLH*), which participate in the brassinosteroid signaling pathway to promote cell elongation of the ligular region (Makarevitch et al., 2012; Tian et al., 2019; Cao et al., 2020; Ren et al., 2020). In addition, *ACS7* (1-aminocyclopropane-1-carboxylic acid synthase 7) controls ethylene biosynthesis (Li et al., 2020), and *LPA1* (*Loose Plant*

## Molecular Plant

*Architecture1*) and *LA1* (*Lazy Plant1*) mediate the leaf gravity response (Dou et al., 2021; Ji et al., 2022), thus playing a crucial role in LA regulation. Although the regulatory roles of these genes are supported by genetic evidence, their spatial expression patterns and regulatory networks within maize plants remain to be clarified. Therefore, a comprehensive investigation into the cellular basis of the ligular region is essential, not only to deepen our understanding of LA regulation but also to identify potential targets for optimizing plant architecture in modern maize breeding.

In recent years, single-cell RNA sequencing (RNA-seq) has emerged as a powerful tool for characterizing cell-type-specific transcriptomes across various tissues (Satterlee et al., 2020; Xu et al., 2021; Han et al., 2023). However, single-cell RNA-seq often struggles to obtain reliable transcriptome data from fragile plant tissues, which are prone to damage during sample preparation (Ding et al., 2020). By contrast, the recently developed single-nucleus RNA-seq (snRNA-seq) technique reduces the negative effects of dissociation or external stimuli, offering a more accurate and reliable reflection of *in vivo* conditions (Ding et al., 2020; Marand et al., 2021; Sun et al., 2022). In this study, we combined bulk RNA-seq with snRNA-seq and comparative histological and cellular analyses to characterize previously undefined cell types and cellular processes in the ligular regions. We identified two atypical basic-helix-loop-helix (bHLH) transcription factors, bHLH30 and its homolog bHLH155, that are specifically expressed in the ligular region and associate with the promoter regions of maize *alpha expansin 5* (*EXPA5*) and *phenylalanine ammonia lyase 7* (*PAL7*), activating their transcription and thereby promoting LA expansion. Overall, we have generated a comprehensive, high-resolution transcriptomic atlas of the ligular region at the single-cell level, reconstructed the developmental trajectory of distinct cell types, and identified numerous potential targets for the regulation of LA in maize.

## RESULTS

### Distribution pattern of SCs in the ligular region

To investigate the cellular basis of LA formation, we selected six representative maize inbred lines with distinct plant architectures and performed comparative histological analyses of the midrib in the blade, sheath, and ligular region. Significant differences among these six inbred lines occurred primarily in the LM regions (Figure 1A; Supplemental Figure 1). Z58, known as a compact inbred line, is the maternal progenitor of ZhengDan958, the most successful hybrid variety in China from 2000 to 2010. Compact-type plants (Z58 and 986) displayed two rows of hypodermal sclerenchyma cells (SCs) with marked lignin deposition, aligned in parallel on both the adaxial (SC1) and abaxial (SC2) sides, and were thus defined as a typical double-track SC pattern. Intermediate-type plants (B73) also displayed a double-track SC pattern with lignin deposition. However, a distinct disconnection comprising 4 to 5 layers of hypodermal cells without lignin was observed in SC1 of B73 plants, and they were thus defined as an atypical double-track SC pattern. Flat-type plants (W22, S115, and S10) exhibited two rows of elongated hypodermal cells on both the adaxial and abaxial sides, with lignin observed only at SC2, a pattern referred to as single-track SC (Figure 1A). Further analysis revealed that Z58 exhibited the shortest cell length in SC1 and the lowest

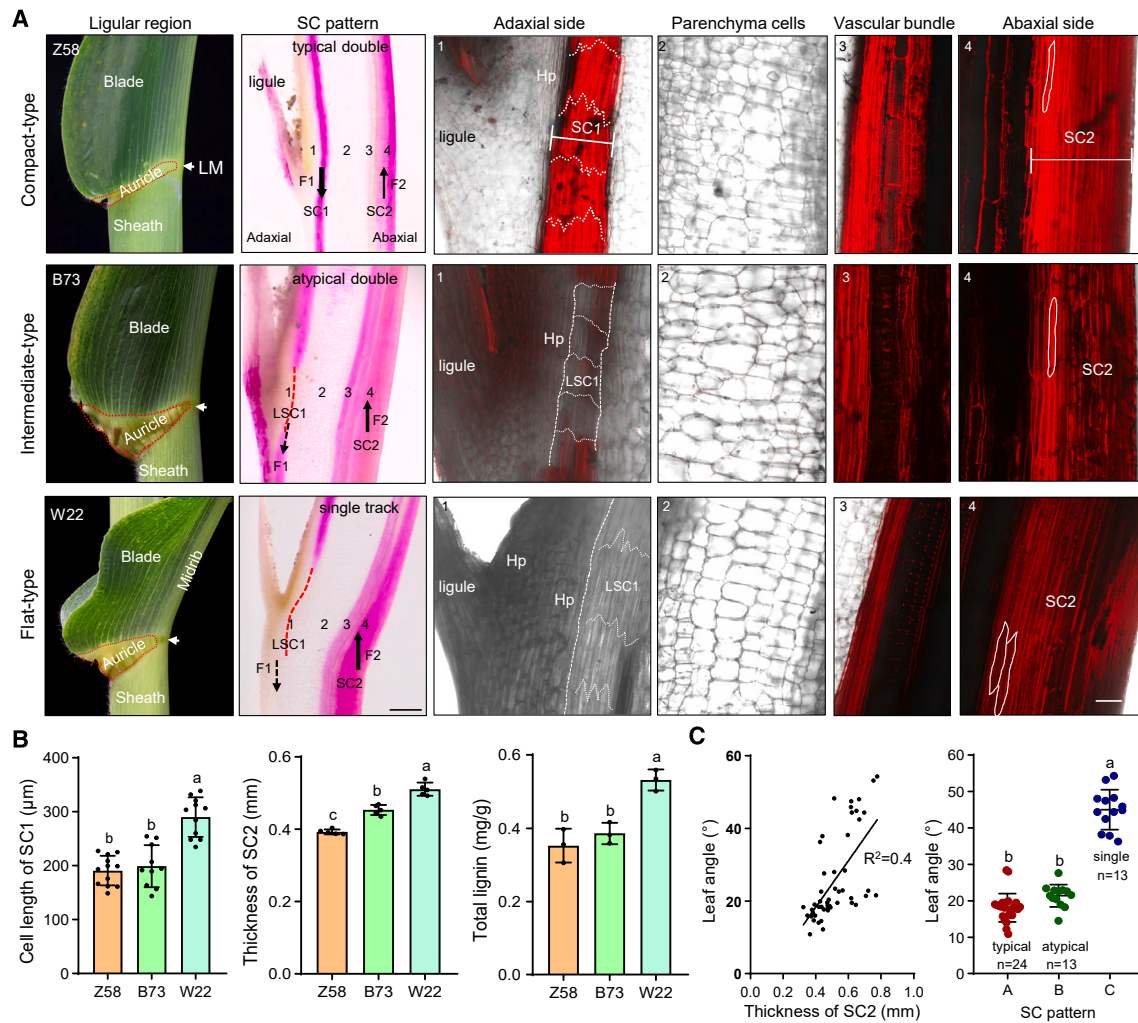


**Figure 1. Comparative histological analysis of the ligular region in various inbred lines.**

(A) Morphological and histological analyses of the ligular region in various maize inbred lines at the tasseling stage. The images in the right four columns represent magnified views of the corresponding areas (labeled 1–4) in the column second from the left. Lignin was visualized by safranin O staining (column second from the left) or lignin auto-fluorescence (right four columns). Hp, hypodermal cells; PC, parenchymal cells; SC, sclerenchyma cells; LSC1, low lignin-deposited SC1. F1, force restricting extension. F2, force supporting erectness. Scale bars, 1 mm for images in the column second from the left and 100 μm for images in the right four columns, respectively.

(B) Quantitative measurement of cell length of SC1 (left), thickness of SC2 (middle), and lignin contents of the LM region (right) in various inbred lines.

(C) Correlation analyses between LA and SC2 thickness (left) and between LA and SC pattern (right) across a population of 50 inbred lines. Each dot in the scatterplot represents an individual inbred line. Bars labeled with different letters represent statistically significant differences, as determined by one-way ANOVA with Tukey's test.

thickness in SC2, consistent with its smallest LA (Figure 1B). Compact- and intermediate-type plants had lignin deposition on both sides; flat-type plants exhibited lignin deposition only on the abaxial side; and total lignin content was highest in the flat-type plants (Figure 1B). Although scattered lignin could be observed in adaxial cells in the midrib of the blade and sheath, it was distinct from the obvious lignin deposition in adaxial SC1 of the ligular region (Supplemental Figures 1C and 1D).

To reveal the cellular basis for the distinct SC patterns in various maize plants, we performed histological analyses of the ligular region at the seedling stage. Elongated hypodermal cells were observed in both the abaxial and adaxial sides (second leaf), and obvious lignin deposition occurred earlier in the abaxial

cells, particularly in B73 and W22 plants. Interestingly, Z58 plants had a shorter adaxial meristematic zone and significantly shorter hypodermal cell length compared with B73 and W22 plants (Supplemental Figure 2). These results revealed that the specialization of SCs is distinct in the adaxial and abaxial regions. At the late stage, Z58 and B73 plants exhibited lignin deposition in the adaxial cells, which restricted elongation and thus caused a small LA. By contrast, W22 plants lacked lignin deposition, failed to restrict adaxial elongation, and thus had a large LA (Figure 1A). The distinct SC pattern extended from the bottom to the flag leaves and was consistent throughout all growth stages in various maize plants (Supplemental Figure 3). Together, all these results revealed that distinct SC patterns in the ligular region are critical for LA formation in various maize plants.

### Specialized SC1 in the ligular adaxial region determines LA size

To investigate whether ligular SCs are correlated with LA, 50 representative lines were randomly selected for histological analyses from a population of 147 inbred lines with LAs ranging from 10° to 60° (Supplemental Table 1). Multiple previous studies have used variation in SC2 thickness to explain LA size in various mutants or inbred lines of maize (Cao et al., 2022). However, only some of the inbred lines analyzed here (Z58, 986, S10, S115) exhibited a positive correlation between SC2 thickness and LA, and others (yun87, Qi205, CML69) exhibited the opposite pattern (Supplemental Figures 4A–4C). Statistical analysis revealed that SC2 thickness was only weakly correlated ( $R^2 = 0.4$ ) with LA in the various maize inbred lines (Figure 1C).

By contrast, inbred lines with visible lignin deposition at SC1, encompassing both typical and atypical double-track SCs, correlated strongly with small LAs (~10°–30°), whereas inbred lines that lacked lignin deposition in the adaxial hypodermal cells (single-track SCs) corresponded to large LAs (~35°–55°). This result indicated a significant negative correlation between LA and lignin deposition in adaxial SC1 (Figure 1C; Supplemental Figures 4A–4C). However, the relationship between LA and the number of cell layers in the adaxial region remains unclear. Our findings suggest that enhanced SC1 is the primary factor leading to narrower LA, probably by restricting adaxial cell elongation and enhancing the mechanical strength of the midrib (Figure 1A, indicated by F1). We also proposed that SC2 may play a role in influencing overall rigidity and mechanical strength, which are necessary to maintain blade erectness (Figure 1A, indicated by F2). Indeed, a comprehensive correlation analysis of LA with other traits across 147 inbred lines revealed that the blade weight ( $R^2 = 0.44$ ), length ( $R^2 = 0.32$ ), and width ( $R^2 = 0.29$ ) were all positively correlated with LA (Supplemental Figure 5).

### Identification of enriched genes in the ligular adaxial region

To investigate the cellular basis and enriched genes mediating the maintenance of the ligular region, we performed bulk transcriptome analyses (RNA-seq) of the LM region in various inbred lines (Z58, B73, W22) at the tasseling stage. We divided the adaxial and abaxial sides of the LM equally from the center region, as shown in Figure 2A, and processed three replicates for each line, generating 18 libraries for comparative RNA-seq analysis. Principal-component analysis showed that these 18 samples clustered into six distinct groups, with high consistency observed within the replicates of each inbred line (Figure 2B). We identified differentially expressed genes using a fold change (FC) of at least 2 and a  $p$  value of 0.05 or less (Figure 2C), revealing 2167, 2884, and 2771 genes that were significantly enriched on the adaxial side of the ligular region in Z58, B73, and W22, respectively. By overlapping these three datasets, we identified 916 genes common to all three lines, which we considered to be adaxially enriched genes. Similarly, we identified 755 abaxially enriched genes across the three inbred lines (Supplemental Tables 2 and 3). Gene Ontology (GO) analysis revealed that the adaxially enriched genes were associated with cell expansion and cell wall organization, whereas the abaxially enriched genes were related to xylem, phloem, and transport of sugar and nutrients (Supplemental Figure 6). These findings underscore the distinct cellular

functions of the ligular adaxial and abaxial sides and confirm the reliability of our bulk RNA-seq results for further analyses.

W22 plants exhibited significantly longer adaxial hypodermal cells compared with Z58 and B73, suggesting the higher expression of cell-elongation-related genes on the adaxial side of W22. To identify these genes, expression values on the adaxial side of W22 were compared with those of Z58 (W22-ad vs. Z58-ad, 2981) and B73 (W22-ad vs. B73-ad, 2563) and then aligned with the core adaxially enriched genes (916). Ultimately, 97 genes were identified as cell-elongation-related genes on the ligular adaxial side and were primarily involved in cellular processes such as cell expansion (*EXPA5*) and cell wall organization (*xyloglucan endo-transglycosylase/hydrolase 4*, *XTH4*) (Figure 2D; Supplemental Table 4).

Z58 and B73 exhibit greater lignin deposition on the adaxial side compared with W22, suggesting enhanced expression of genes related to cell lignification of SC1 on the adaxial side of Z58 and B73 and, similarly, on the abaxial side of W22. To investigate this further, we performed a comparative analysis of gene expression levels between the adaxial sides of Z58 and W22 (Z58-ad vs. W22-ad, 2766) and B73 and W22 (B73-ad vs. W22-ad, 3023) and between the abaxial and adaxial sides of W22 (W22-ab vs. W22-ad, 2237). Finally, 326 candidate genes that were potentially involved in cell lignification were identified (Figure 2D; Supplemental Table 5). Multiple genes associated with lignin monomer biosynthesis (*cinnamyl alcohol dehydrogenase 8B*, *CAD8B*), transport (*ABC transporter G family member ABCG6/14*), and polymerization processes (*peroxidase 45*, *PRX45*) were further validated by RT-qPCR (Figures 2D–2F; Supplemental Figure 7). A number of genes associated with secondary cell-wall biosynthesis (*cellulose synthase 12*, *CESA12*) and the Caspary strip (*CASP9*) were also identified. A variety of transcription factors probably related to the cellular processes of cell elongation or lignification, including *bHLH29/30/62/155*, *NAC16/47/132*, and *MYB37*, were identified as potential novel regulators in LA maintenance (Figures 2C and 2D; Supplemental Table 6).

### Single-nucleus transcriptome analysis of the ligular region

To investigate the distinct cell types and enriched genes in the ligular region at a single-nucleus resolution, we performed an snRNA-seq analysis of the ligular region (second leaf, V3) in plants of the elite inbred line Z58. We performed both longitudinal and cross-sectional analyses of the ligular region to identify distinct cell types and developmental stages (Figures 3A and 3B). Ultimately, we obtained a high-quality, comprehensive transcriptomic atlas of the ligular region, consisting of 7049 nuclei. The maximum number of unique molecule identifier counts in a single nucleus was 1729, and the median and minimum unique molecule identifier counts per nucleus were 1128 and 732, respectively (Supplemental Table 7). In total, 23 657 genes were detected in the ligular region, accounting for 60% of the predicted genes in the B73 reference genome (v.4). We used uniform manifold approximation and projection (UMAP) for dimensionality reduction and visualization and ultimately identified 16 putative cell clusters (C0–C15) in the ligular region (Figure 3C).

To annotate these distinct cell clusters, we first explored the expression profiles of adaxially and abaxially enriched genes

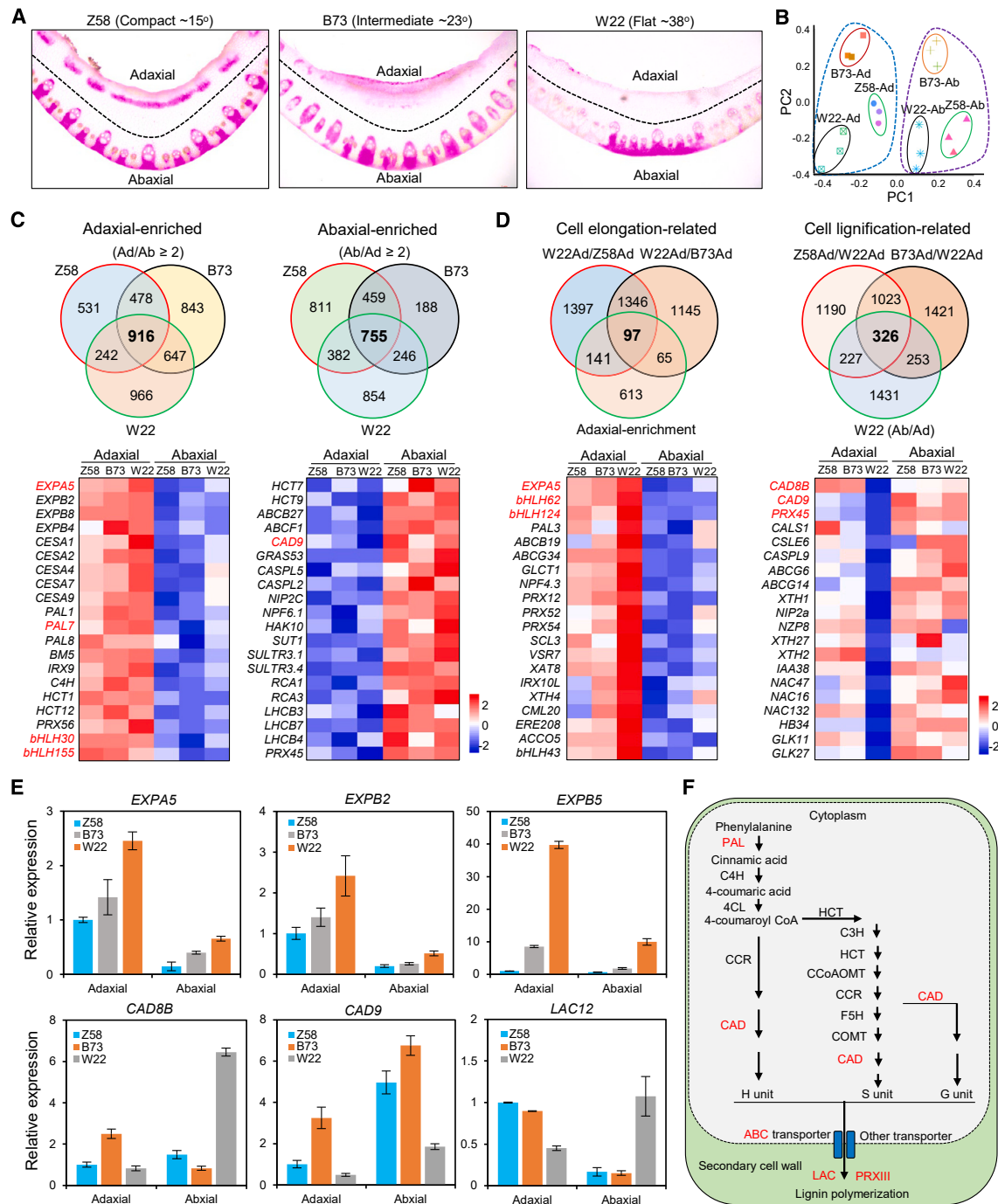


**Figure 2. Comparative transcriptome analysis of the LM region in various inbred lines.**

(A) Histological analysis of the ligular adaxial and abaxial sides. Lignin was visualized by safranin O staining. Dashed lines indicate the position that divides the LM into two parts for RNA-seq.

(B) Principal-component analysis of 18 bulk RNA-seq datasets.

(C and D) Venn diagrams (top) and heatmaps (bottom) show the number and specific genes enriched on the adaxial or abaxial side (C) or related to cell elongation and lignification on the ligular adaxial side (D), respectively.

(E) RT-qPCR analyses verified the expression profiles of the identified differentially expressed genes in RNA-seq.

(F) A diagram showing genes related to lignin biosynthesis and polymerization, with those altered in various plants highlighted in red.

in the snRNA-seq results. Adaxially enriched genes were primarily expressed in clusters C5, C6, C9, C10, and C11, and abaxially enriched genes were primarily expressed in clusters C7, C8, C13, C14, and C15 (Supplemental Figure 8). Taking

advantage of distinct cell-specific markers and their expression profiles on the UMAP, we successfully annotated most of the cell clusters (Figures 3C and 3D; Supplemental Table 8). For instance, in cluster C10, we observed enrichment of epidermal

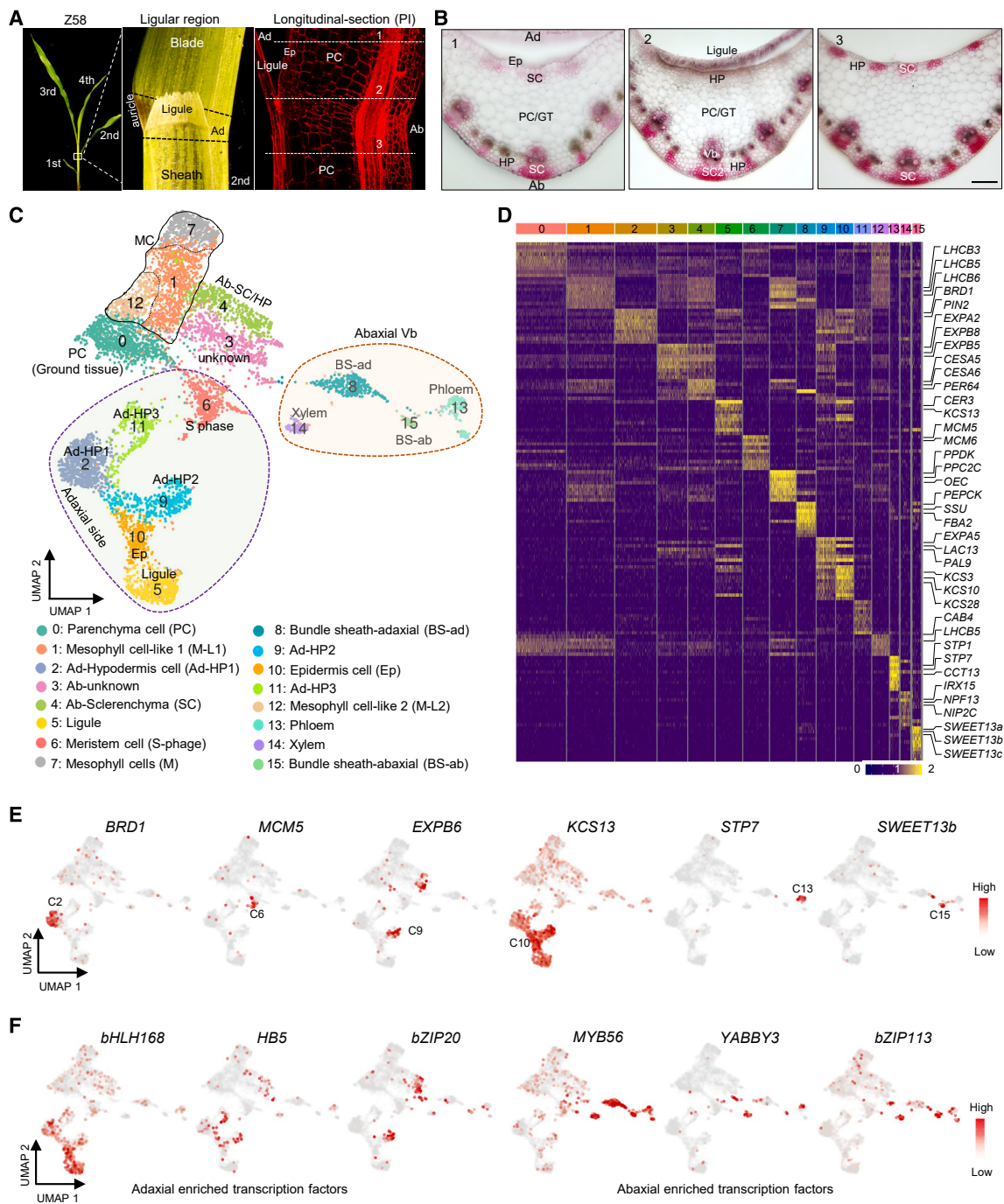


**Figure 3. Single-nucleus transcriptome reveals cell heterogeneity in the ligular region.**

(A) Morphological and histological analyses of the ligular region (second leaf, V3, Z58) for snRNA-seq. The longitudinal section was stained with propidium iodide to highlight different cell types.

(B) Cross-section analyses of the LM at the positions indicated in (A). Lignin was visualized by safranin O staining. Hp, hypodermal cells; PC, parenchymal cells; SC, sclerenchyma cells. Scale bar, 0.5 mm.

(C) UMAP visualization depicting distinct cell clusters in the ligular region.

(D) Heatmap showing the expression profiles of various cell-type marker genes across 16 identified cell types.

(E and F) Expression profiles of specific marker genes (E) and transcription factors (F) in the ligular region.

cell markers such as *Glossy1* and *3-Ketoacyl-CoA synthase* (*KCS3/10/13/28*), indicating that this cluster represents epidermal cells. *KCS13*, *CER3*, and *lanosterol synthase 1* (*LAS1*) were also highly expressed in C2, C5, and C9, suggest-

ing that these clusters might represent cell types connected to epidermal cells. Mitosis (S-phase)-related genes, including *Minichromosome Maintenance 5* (*MCM5*) and *MCM6*, were highly expressed in cluster C6, indicating that it might represent cells

in the adaxial meristematic zone (Figures 3C–3E; Supplemental Figure 9).

In the abaxial clusters, *irregular xylem protein (IRX15)* and *nitrate transporter/peptide transporter (NPF13)* were enriched in C14, indicating that this cluster represented xylem, and sucrose transporter genes (*STP1/7*) and *phloem protein 2-like* were enriched in C13, indicating that it represented companion cells (phloem). Multiple *amino acid/auxin permeases (AAP6/8)* and *sugars will eventually be exported transporter (SWEET13a/b/c)* were enriched in C15, indicating that it represented the bundle sheath (BS) abaxial cells. Multiple Calvin-cycle-related genes, including *Rubisco small subunit (SSU)*, *malic enzyme 3 (ME3)*, *fructose-bisphosphate aldolase 2 (FBA2)*, and *Rubisco activase 1 (RCA1)*, were significantly enriched in C8, indicating that it represented BS cells. Multiple photosystem II genes such as *Lhcb3/B5/B6* and *oxygen-evolving complex (OEC)* subunits were identified in C7, indicating that it represented mesophyll cells. Interestingly, C1 and C12 contained highly enriched C3 and C4 pathway-related genes in the single-type cells, which were distinct from the common mesophyll and BS cells in the blade, indicating that they might represent undefined cell types exhibiting a novel type of photosynthesis in maize (Figures 3C–3E; Supplemental Figure 9).

Interestingly, our annotation revealed that the ligular region exhibited distinct cell types compared with the blade, stem, and root (Figures 3A and 3B). Although multiple layers of elongated hypodermal cells, similar to those in the cortex and endodermis, were observed on both the adaxial and abaxial sides, their identity remains difficult to verify owing to the absence of multiple classical marker genes for cortical and endodermal cells. Consequently, we classified them as distinct types of hypodermal cells (HP1–3) (Figures 3C and 3D). Multiple plant-hormone-related genes including *BRD1* and *PIN-formed protein (PIN2)* were enriched in C2, indicating that this cluster represents one kind of adaxial hypodermal cell (Ad-HP1) and plays a crucial part in ligular maintenance by mediating hormone signaling pathway(s) (Figure 3E).

To identify clusters related to hypodermal SCs, we focused on the expression profiles of elongation- and lignification-related genes. We discovered that elongation-related genes such as *EXPs*, *auxin response factor (ARFs)*, and *auxin/indole-3-acetic acid (Aux/IAAs)* were enriched in clusters C3, C4, and C9 and that lignin monomer biosynthesis and polymerization (*PRX*) genes were enriched in clusters C3, C4, C9, and C11 (Figures 3D and 3E; Supplemental Figure 10). On the basis of their expression profiles and positions in the UMAP, clusters C9 and C11 were annotated as Ad-HP2 and Ad-HP3, respectively, which undergo elongation and lignification related to adaxial SC1. Clusters C3 and C4 represent abaxial HP cells related to SC2.

We next investigated the expression profiles of multiple key LA regulators using UMAP (Figures 3F; Supplemental Figures 11 and 12). LG1 and LG2, two well-documented key regulators of LA, were weakly expressed in the snRNA-seq data of the ligular region (Supplemental Figure 12), consistent with their crucial roles in the early stages of ligular development, particularly in establishing the sheath-blade boundary and PLB. Other well-known regulators, such as *BRD1*, *BZR1*, *BEH1*, *TAC1*, *DWF4*, and *bHLH112*, were detected in our snRNA-seq results. Intriguingly, we identified

## Function of sclerenchyma cells in leaf angle regulation

several potential novel regulators of LA, such as the transcription factors *bHLH124/165/168* and *HB5/22/53*, which were enriched in adaxial cells, whereas *MYB6/8/56*, *YABBY3/11/15*, and *bZIP113* were enriched in abaxial cells (Figure 3F; Supplemental Table 9). All these findings further validated our snRNA-seq analysis of the ligular region in maize.

## Reconstructing the developmental trajectory of the ligular adaxial cells

Given that our snRNA-seq assay captured and sequenced over 7000 nuclei at different states, it can facilitate the exploration of cell developmental trajectories. To reveal the cellular basis and developmental trajectory of adaxial SCs, we selected 2706 adaxial-side nuclei (clusters 2, 5, 6, 9, 10, and 11) for pseudotime analysis (Figure 4A). As shown in Figure 4B, meristem cells (C6) were enriched at the beginning of the pseudotime, Ad-HP1 (C2) cells were predominant at the first branch point, and Ad-HP2 (C9), Ad-HP3 (C11), ligule (C5), and epidermal (C10) cells were distinctly concentrated at three different endpoints, indicating that these cells are highly differentiated. All these results verified the developmental trajectory of adaxial SCs in the ligular region.

To reveal genes involved in spatiotemporal regulation of the ligular region, 3391 genes were identified that were significantly correlated with pseudotime progression. As shown in Figure 4C, prebranch 1 bifurcated into two distinct orientations. GO enrichment analyses revealed that cell fate 1 (C11) was enriched with genes involved in defense, external stimulus, and lignin biosynthesis, whereas cell fate 2 was enriched with genes related to the lipid biosynthetic process, hormones, cell wall biogenesis, and cell differentiation. Prebranch 2 split into two distinct orientations (C9 and C5/C10). Among the genes in cell fate 3, genes related to cell expansion (*EXPs*), cellulose biosynthesis (*CESAs*), and lignin biosynthesis (*PALs*) were enriched, and these were also highly expressed in cluster C9 (Figures 4C–4E; Supplemental Figure 13; Supplemental Table 10). Importantly, multiple transcription factors, including *bHLH30* and *bHLH155*, were identified as putative key regulators mediating cell elongation and lignin biosynthesis in adaxial SCs (Figures 4D and 4E), suggesting that these putative regulators may play a crucial role in the regulation of ligular adaxial cells.

## Maize *bHLH30* and *bHLH155* positively regulate LA expansion

To validate the biological functions of these putative regulators, we initially checked whether they were located within various QTL or genome-wide association study peaks identified in previous studies of LA (Tian et al., 2011; Ku et al., 2012; Dzievit et al., 2019; Peng et al., 2021; Duan et al., 2022; Zhao et al., 2022; Li et al., 2023; Zhu et al., 2023). We found that maize *bHLH30* was located in a QTL for LA but had not been functionally characterized (Duan et al., 2022). Multiple sequence alignment revealed that maize *bHLH30* and its closest homolog, *bHLH155*, encoded two atypical bHLH transcription factors, less than 100 aa in length, with a less conserved basic region at the N terminus and thus did not directly bind DNA (Supplemental Figure 14). Collinearity analysis among maize, teosinte, and other grass plants revealed that *bHLH155* was duplicated from *bHLH30*, suggesting that they may play redundant regulatory roles in the maintenance of LA in maize (Supplemental Figure 15).

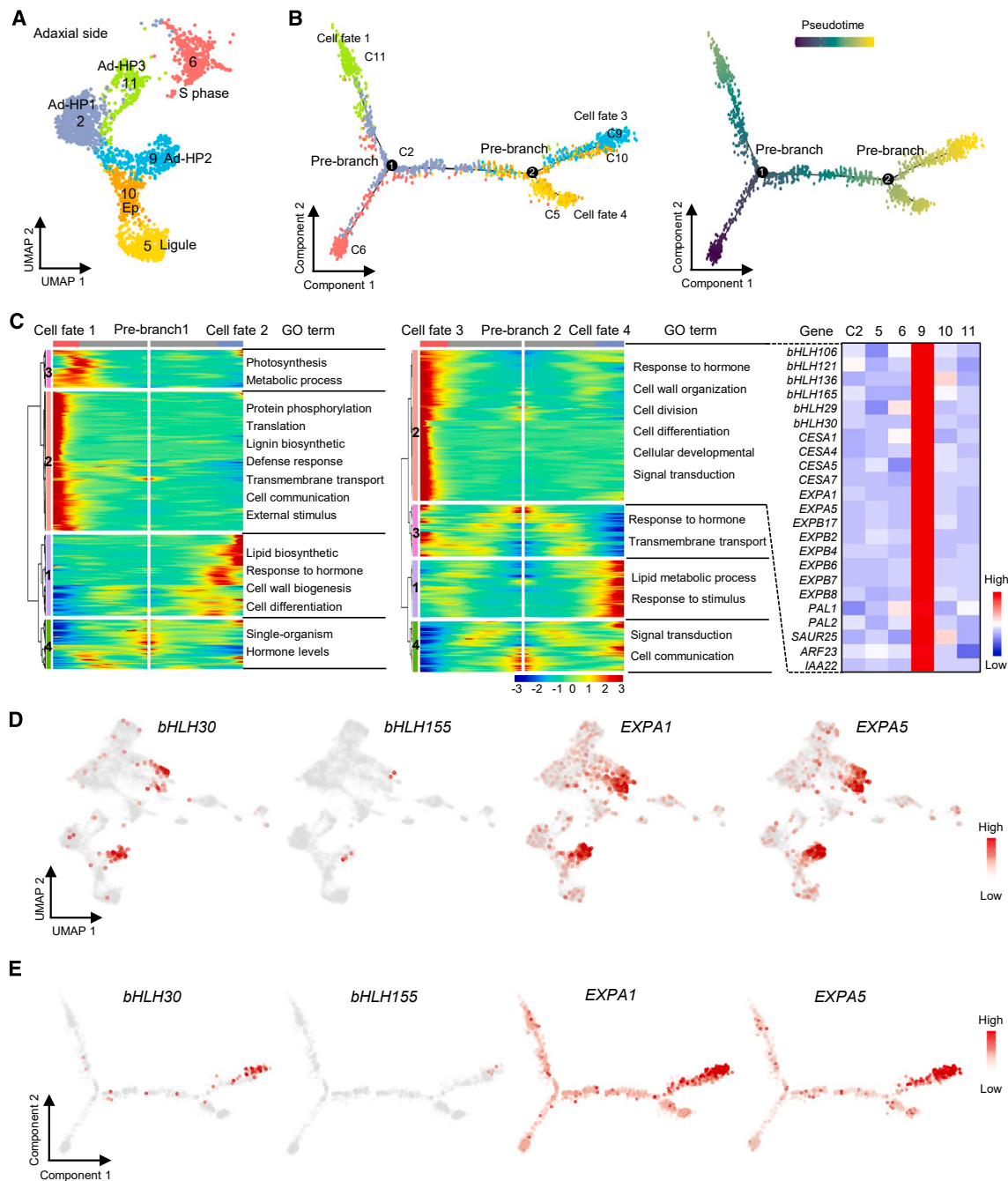


**Figure 4. Developmental trajectory analyses of the ligular adaxial cells.**

(A) UMAP visualization highlighting distinct cell types of the adaxial side for pseudotime analysis.  
(B) Pseudotime trajectory analysis of the LM adaxial cells (left), with colors indicating different stages of inferred pseudotime (right).  
(C) Heatmap showing the expression profiles of the branch-dependent genes across pseudotime. Both ends of the heatmap correspond to the extremities of pseudotime. Representative GO terms for each gene cluster are shown. The right image shows the representative genes in cluster 2 (pre-branch 2) and their expression profiles in distinct adaxial cell clusters. The color bar indicates the relative expression level.  
(D and E) Expression profiles (D) and developmental trajectories (E) of selected genes related to cell elongation on the adaxial side.

To investigate the spatial expression patterns of *bHLH30* and *bHLH155*, we performed RT-qPCR analyses, which verified their high expression in the ligular region (Supplemental Figure 16A). Further exploration through RNA *in situ* hybridization assays revealed that, compared with sense probes, the antisense probes of maize *bHLH30* and *bHLH155* were detected in the ligular

region, particularly within the adaxial and abaxial hypodermal cells and SCs, consistent with our snRNA-seq results (Supplemental Figure 16B). To further explore their physiological functions in maize, we generated null alleles for both genes in the KN5585 inbred line background using CRISPR/Cas9 genome-editing technology (Figure 5A). Compared with KN5585 plants, the

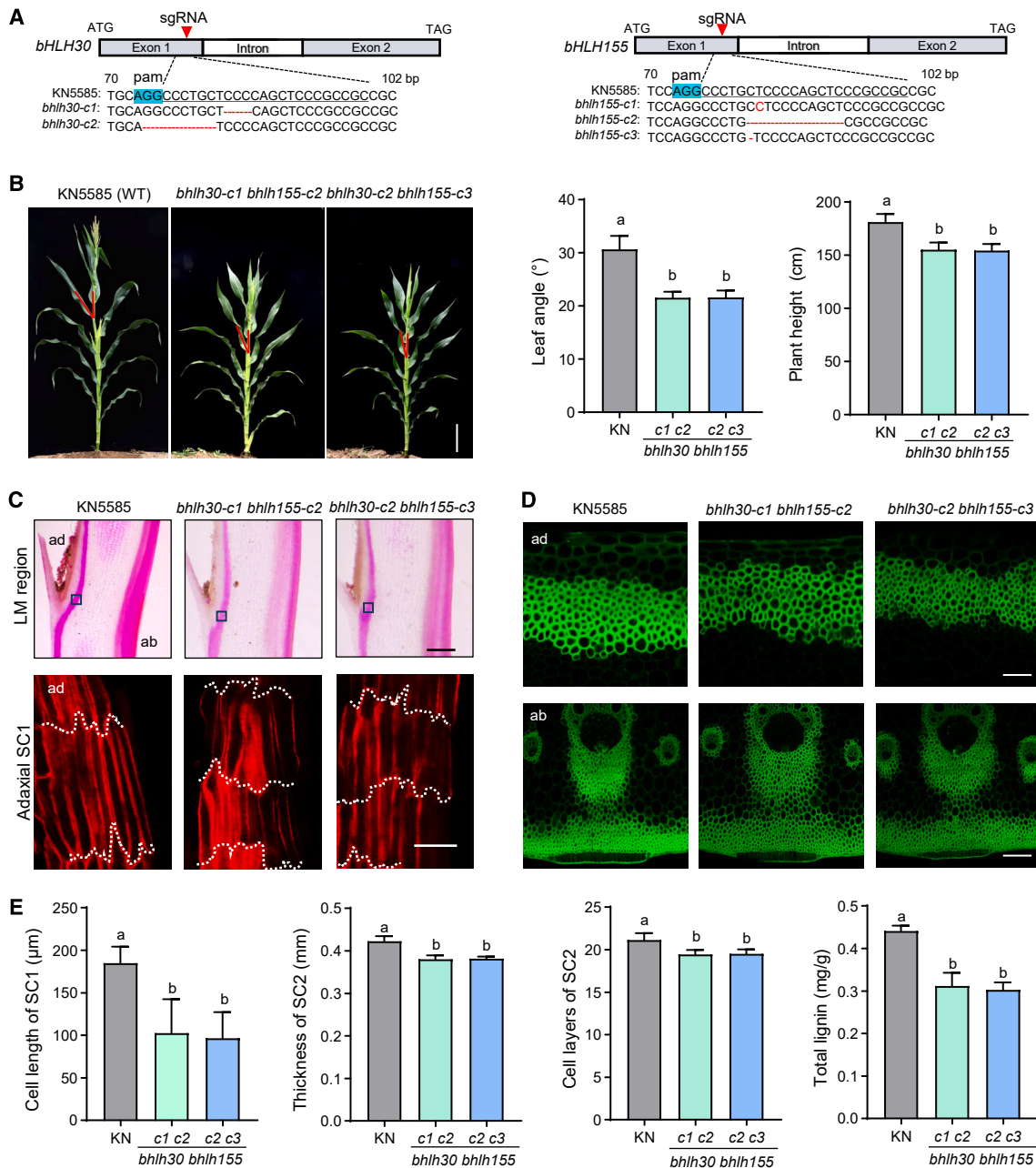


**Figure 5. Maize *bHLH30* and *bHLH155* positively regulate LA expansion.**

- (A) Generation of maize *bHLH30* and *bHLH155* mutants in the KN5585 inbred line (wild type) background using CRISPR–Cas9 technology.
- (B) Morphological analysis (left) and quantitative measurements (right) of LA and PH in various plants at the tasseling stage.
- (C) Longitudinal sections of the LM region (top) and magnified view (bottom) of the adaxial SC1. Scale bars, 1 mm (top) and 100 μm (bottom).
- (D) Auto-fluorescence imaging of lignin in the adaxial SC1 (top) and abaxial SC2 (bottom). Scale bar, 100 μm.
- (E) Quantitative analysis of the cell length in SC1 (left), thickness and number of cell layers in SC2 (middle two images), and total lignin in the LM region (right) across various plants. Statistically significant differences determined by one-way ANOVA with Tukey's test are denoted by different letters.

various mutants had significantly reduced LA and plant height (PH), especially the *bhlh30 bhlh155* double mutants (Figure 5B; Supplemental Figure 17). Histological analyses revealed that the cell length of SC1 and the thickness and cell layers of SC2 were significantly reduced in various mutants. Safranin O staining, lignin auto-fluorescence, and total lignin measurement all verified that the *bhlh30*, *bhlh155*, and *bhlh30 bhlh155* mutants had a significantly lower content of total lignin (Figures 5C–5E;

Supplemental Figure 17). All these results suggested that *bHLH30* and *bHLH155* positively regulate LA expansion by directly promoting cell expansion and lignin deposition.

#### Identification of *bHLH30* and *bHLH155* targets in the ligular region

To further characterize the physiological function of *bHLH155*, we generated its overexpression (OE) line *bHLH155-OE* in the Z58

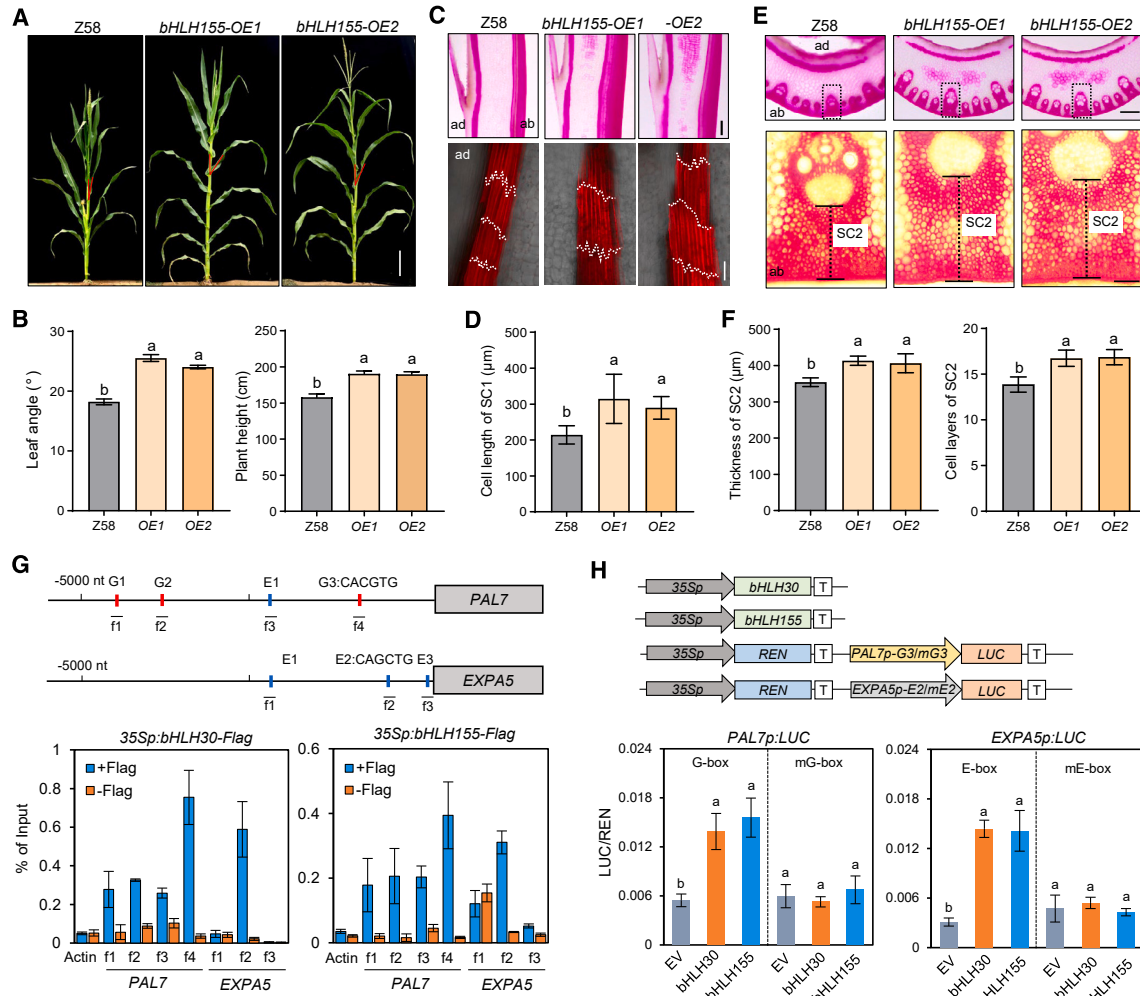


**Figure 6.** *bHLH30* and *bHLH155* promote cell elongation and lignin biosynthesis.

(A and B) Morphology (A) and measurement (B) of *bHLH155-OE* lines at the tasseling stage. Scale bar, 20 cm.

(C and D) Longitudinal sections (C) and measurement (D) of the adaxial SC1 in various plants. Scale bars, 1 mm (top) and 100  $\mu\text{m}$  (bottom).

(E and F) Cross-sections (E) and measurement (F) of the abaxial SC2 in various plants. Scale bars, 1 mm (top) and 100  $\mu\text{m}$  (bottom).

(G) ChIP-qPCR assay showing that *bHLH30* and *bHLH155* associate with the promoter regions of *PAL7* and *EXPA5*.

(H) Transient expression assay showing that *bHLH30* and *bHLH155* promote the transcription of *PAL7* and *EXPA5* through the G-box or E-box *cis*-elements but not mutated *cis*-elements. Different letters above bars represent significant differences determined by one-way ANOVA with Tukey's test.

background. Compared with Z58 plants, *bHLH155-OE* plants exhibited a larger LA and greater PH (Figures 6A and 6B). Histological analyses showed that the cell length of SC1 and the thickness and cell layers of SC2 were significantly greater in *bHLH155-OE* plants than in Z58 plants (Figures 6C–6F). These genetic and histological results confirmed that *bHLH155* plays a positive role in establishing LA. RT-qPCR analyses showed that the transcript levels of multiple elongation- and lignification-related genes were significantly lower in *bhlh30* *bhlh155* mutants but upregulated in *bHLH155-OE* plants compared with wild-type control plants (Supplemental Figure 18). Analysis of promoter sequences revealed multiple G-box or E-box *cis*-elements in the promoter regions of *PAL7* and *EXPA5*, suggesting that they might be targets of *bHLH30* and *bHLH155*, and this was verified by chromatin immunoprecipitation (ChIP)-qPCR assays in maize protoplasts (Figure 6G). Transient expression assays revealed that *bHLH30* and *bHLH155* significantly increased the activities of luciferase (*LUC*) reporters driven by

*PAL7* or *EXPA5* promoters but failed to activate *LUC* reporters driven by mutated promoters (Figure 6H). All these molecular results revealed that both *bHLH30* and *bHLH155* activate the transcription of cell-elongation- and lignification-related genes. Because both *bHLH30* and *bHLH155* encode atypical bHLH transcription factors that do not directly bind DNA, it is possible that they activate the expression of targets by interacting with other typical bHLH (or other type) transcription factors that are specifically co-expressed in the same cell type.

## DISCUSSION

LA is a pivotal trait in crop plants, determining compactness, planting density, and yield. The regulation of LA has been proposed to be largely conserved among cereals such as maize, rice, and wheat, highlighting its significance in agricultural research. In rice, multiple previous studies have demonstrated that asymmetric cell proliferation and elongation on the

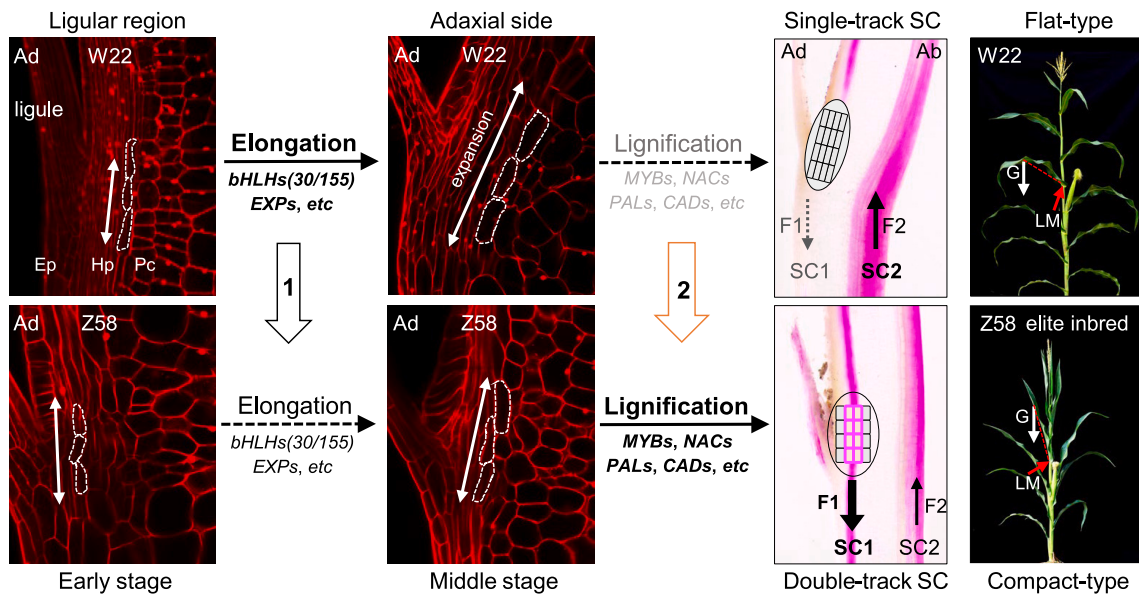


**Figure 7. Specialization of SCs promotes LA narrowing.**

The diagram shows a two-step regulatory process influencing the regulation of LA: initial cell elongation (step 1) followed by cell lignification (step 2) on the ligular adaxial side. In flat inbred lines (e.g., W22), enhanced elongation, coupled with a deficiency in lignification (single-track SCs), results in an increased LA and flatter plant architecture (top). Conversely, in compact inbred lines (e.g., Z58), reduced elongation and enhanced lignification (double-track SCs) of the adaxial cells lead to a smaller LA and more compact plant architecture (bottom). Bold font and lines highlight an enhanced step; gray font and dashed lines indicate a weakened step. SC, sclerenchyma cells; G, the gravitational force acting on the leaf blade; F1, the force restricting extension and bending away of the blade; F2, the support force from the sheath to the leaf blade.

adaxial or abaxial side of the lamina joint determine the LA (Zhou et al., 2017). In maize, the ligular region, similar to the lamina joint in rice, has been considered the primary regulatory region for LA (Kong et al., 2017). Given the morphological differences between maize and rice leaves, with maize leaves being longer, broader, larger, and heavier, it is plausible that maize might evolve a different regulatory mechanism for LA.

Our study revealed a two-step regulatory process involving initial cell elongation and subsequent enhanced lignification in the ligular adaxial SCs that plays a crucial role in restricting LA expansion (Figure 7). SCs are a specialized tissue known for providing rigidity and structure and are closely linked to lodging and disease resistance (Wang et al., 2020b; Shah et al., 2021). Previous studies have focused primarily on the abaxial SC2 in the ligular region to explain LA variation in rice, maize, and other crops (Wang et al., 2022). After a systematic comparison of various maize inbred lines, we found that SC2 exhibited only a weak correlation with, but did not directly determine, LA. Strikingly, we found that lignin deposition on the adaxial SC1 plays a predominant role in restricting LA expansion, as increased lignin deposition restricts expansion of the adaxial hypodermal cells (Figure 1; Supplemental Figures 1–4). These findings emphasize the significance of adaxial SC1 in providing mechanical strength and limiting adaxial elongation during LA regulation, which is distinct from the regulatory mechanisms in rice or other crop plants. Our findings also revealed that the orientation of leaf blades is primarily influenced by a dynamic equilibrium between the downward force of gravity on the blade and the counteracting mechanical strength provided by SCs in the ligular region, highlighting the complex biomechanical

forces that shape plant architecture in maize (Figure 7; Supplemental Figure 19).

To unravel the cellular basis and molecular processes involved in maintenance of the ligular region, we optimized the rapid nucleus isolation procedure and performed an snRNA-seq assay of the ligular region in Z58 plants. Through integration of snRNA-seq and bulk RNA-seq datasets, we identified distinct cell types and generated a comprehensive transcriptomic atlas of the ligular region (Figures 2 and 3). We confirmed the presence of previously identified key regulators of LA, such as *LG1*, *LG2*, *ACS7*, and *BRD1*, in the specific cell types within the ligular region (Figure 3), confirming the reliability of our snRNA-seq dataset. Our transcriptomic analysis enabled us to identify specific cell types and relevant enriched genes associated with SC1 in the ligular region. We found that SC1 was likely derived from Ad-HP2 and HP3, as supported by its cellular position in the ligular region and the enrichment of endodermal markers, such as Caspian-strip proteins (CASP) and Dirigent proteins, in the adaxial hypodermal cells (Figure 3). These findings suggest that adaxial SC1 may exhibit properties similar to the Caspian strip in roots. The pseudotime trajectory analysis revealed a putative lineage transition in the ligular adaxial cells (Figure 4). Interestingly, although most adaxial hypodermal cells were elongated, only a portion of these cells underwent lignification and specialized into SCs in the different inbred lines. This may be related to the particular expression of CASPs and Dirigent proteins in the specific ligular hypodermal cells, which can directly trigger lignin deposition and SC specialization in *Arabidopsis*.

In addition to identification of distinct cell types in the ligular region, we discovered a set of novel regulators potentially

involved in LA maintenance, including multiple enzymes directly involved in cell elongation and lignification (*EXPs*, *PALs*, *XTHs*, *CESAs*, *Laccases*, *CADs*, and *PRXs*), as well as related transcription factors (*bHLH*, *MYB*, and *NACs*) (Figures 2, 3, and 4). Multiple transcription factors related to cell elongation, such as *IBH1* and *IL1*, have been shown to significantly affect LA (Cao et al., 2020; Ren et al., 2020), but most *MYB* and *NAC* mutants in maize did not exhibit significant alterations in LA phenotype (Liu et al., 2021b). We examined the LA morphology of various mutants related to secondary cell wall biosynthesis, including *brown-midrib* and *brittle stalks* mutants, which are defective in lignin or cellulose biosynthesis. Remarkably, the LA sizes of these mutants were indistinguishable from those of the wild type (data not shown), suggesting that secondary cell wall biosynthesis is essential but is not the primary factor that directly determines LA. This observation implies that the position of lignin deposition, rather than its biosynthesis *per se*, is critical for the specialization of adaxial SC1 and LA size.

To investigate the cellular basis of LA regulation, we focused on the elongation of adaxial SC1. We identified *bHLH30* and its closest homolog, *bHLH155*, as two key regulators promoting cell elongation of SC1, thereby affecting LA regulation. Various mutants lacking functional *bhlh30* and *bhlh155* displayed shorter SC1 cells, leading to a reduced LA (Figure 5). Conversely, OE of *bHLH155* led to enhanced elongation in SC1 and large LAs (Figure 6), supporting our hypothesis that variation in adaxial SC1 largely determines LA (Figure 1). Molecular analyses revealed that *bHLH30* and *bHLH155* activate the transcription of genes related to elongation in the ligular region (Figures 6G and 6H). Although *bHLH30* and *bHLH155* proteins do not bind directly to DNA, they are likely to control the expression of downstream targets by interacting with typical *bHLH* transcription factors. The antagonistic interaction between *HLH/bHLH* pairs, such as *PRE1* and *IBH1* in *Arabidopsis* and *IL1* and *IBH1* in rice, is an evolutionarily conserved regulatory mechanism in cell elongation (Zhang et al., 2009). We noted that maize *bHLH30* and *bHLH155* are closely related to rice *IL1* and *Arabidopsis PRE1*, suggesting that they may interact with maize *IBH1* or other typical *bHLH* transcription factors enriched in the hypodermal cells of the ligular region. In addition, these atypical *bHLH* proteins may interact with other types of transcription factors, including *MYBs* and *NACs*, to coordinately regulate cell lignification in the ligular region, thus affecting LA regulation.

In summary, our study demonstrated that initial elongation and subsequent lignification, a two-step regulatory process in the ligular adaxial SCs, play a critical role in LA regulation. We confirmed the pivotal regulatory role of *bHLH30* and its homolog, *bHLH155*, two atypical *bHLH* transcription factors that govern cell elongation and subsequent lignification of adaxial SC1, thus influencing LA (Figure 7). Finally, we generated a comprehensive transcriptomic atlas of the ligular region at single-nucleus resolution, which not only significantly broadens our understanding of LA regulation but also provides numerous potential targets for achieving desired plant architecture in modern maize breeding.

## METHODS

### Plant materials and growth conditions

A total of 147 maize inbred lines with a range of LA from 10° to 60° in distinct genetic backgrounds were used in this study (Supplemental Table 1). The *bhlh30* and *bhlh155* mutants were generated using CRISPR-Cas9 technology in the KN5585 background by WIMI Biotechnology (Changzhou, China). For genotyping, gene-specific primers were used to amplify the DNA fragment harboring the target sequences, and the PCR products were then sequenced to identify the mutations. After backcrossing with KN5585, the homozygous mutants (T2 and T3) without Cas9 were identified and used for phenotypic analyses. As a result, two null alleles of *bhlh30* (*bhlh30-c1* and *-c2*) and three null alleles of *bhlh155* (*bhlh155-c1*, *-c2*, and *-c3*) were identified. The *bHLH155-OE* transgenic lines were generated in the Z58 inbred line background by EDGENE Biotechnology (Wuhan, China). To identify the *bHLH155-OE* plants, the ligular regions of multiple independent transgenic lines were collected for RNA extraction and RT-qPCR. Transgenic lines with enhanced *bHLH155* expression were further identified through immunoblotting assays. Finally, two independent transgenic lines were self-pollinated to produce homozygous *bHLH155-OE* plants (T2 and T3) for phenotypic analyses.

Maize seedlings for snRNA-seq were grown in growth chambers under a 12-h light/12-h dark cycle at a light intensity of 300 μmol/m<sup>2</sup>/s and a temperature of 25°C. For cytological and bulk RNA-seq analyses of the LM region at the tasseling stage, different inbred lines, various mutants, and the *bHLH155-OE* lines were grown in the summer under field conditions in Taian, Shandong, China (117°06' E, 36°11' N).

### Histological analyses of the LM region

For histological analyses, fresh ligular regions were collected from different plants and cut into free-hand sections. At the seedling stage (V3), longitudinal sections of the ligular region (second leaf) from various plants were stained with propidium iodide (100 μg/ml, 10 s) and examined under a confocal microscope (Zeiss LSM 880). At the tasseling stage, cross and longitudinal sections of the LM region of the leaf above the primary ear collected from various plants were stained with safranin O for 5 min. The sections were then cleared with 75% ethanol and analyzed to assess the distribution pattern of SCs. The thickness of SC2 and the cell length of SC1 in the ligular region were measured using Image J software. Lignin auto-fluorescence was observed by confocal microscopy (LSM 880) with excitation at 300 nm and detection at 400–500 nm.

### RNA sequencing and data analysis

The adaxial and abaxial sides of the LM region in the leaf above the primary ear from three inbred lines (Z58, B73, and W22) were equally divided and used for the bulk RNA-seq assay. Three biological replicates were performed for each inbred line, with the LM region of five individual plants pooled as one replicate. Total RNA was extracted using the Ultrapure RNA kit (CWBIOD, Beijing, China). The quality of the total RNA was checked with a NanoDrop 1000 spectrophotometer. The RNA-seq assay was performed using the DNaseQ-T7 high-throughput sequencing platform by Annoroad Gene Tech (Beijing, China). Approximately 50 million high-quality reads were generated for each sample, resulting in a total of 0.86 billion reads. All reads were mapped to the B73 genome (v.4). Principal-component analysis was performed in R software with default settings to visualize the relatedness among the 18 libraries. Differentially expressed genes were identified based on a FC ≥ 2 or ≤ 0.5, a p ≤ 0.05, and an FPKM (fragments per kilobase of exon model per million mapped reads) ≥ 1 (average FPKM in two different inbred lines). GO enrichment analyses were performed using AgriGO and GO.

### snRNA-seq library preparation and data analysis

The ligular region (L2) of the Z58 inbred line at the V3 stage was used for snRNA-seq. More than 30 fresh ligular-region samples were cut with a

# Molecular Plant

blade and dissolved in extraction buffer for nucleus isolation following a previously described procedure (Song et al., 2023). Nuclear concentration and activity were measured using a hemocytometer and DAPI staining, respectively. DAPI staining confirmed that over 90% of the nuclei were live, and they were then subjected to snRNA-seq analysis. The snRNA-seq library was prepared using the BMKMANU DG1000 Library Construction Kit and sequenced on the Illumina NovaSeq 6000 platform by Annoroad Gene Tech. After removal of low-quality reads and adapters, the clean data were mapped to the maize B73 genome (v.4) using STAR software. The resulting data were used as input files for Seurat (v.4.3.0.1) to perform further quality control and analysis. The expression matrix of the single-cell transcriptome was generated, and genes (at least 200 genes) and cells (at least 3 cells) were filtered. A total of 7049 cell nuclei with high-quality results were retained. Clustering of cells was performed using the FindClusters function, and the results were presented in a two-dimensional UMAP. Monocle (v.2) was used for in-depth analysis of cell developmental trajectories and cell fate determination. Cell-type-specific marker genes were identified by comparing the expression values of various genes in each cluster against all other clusters using the FindAllMarkers function.

## RNA *in situ* hybridization

The ligular region (L2) of the Z58 inbred line at the V3 stage was used for RNA *in situ* hybridization of *bHLH30* and *bHLH155*. The ligular regions were selected and fixed in formaldehyde, alcohol, and acetic acid overnight at 4°C. The sample was embedded in paraffin after being dehydrated with ethanol, cleared with xylene, and sectioned at 10 µm (Thermo Scientific HM 355S). RNA *in situ* hybridization was performed as described previously (Song et al., 2023). Images were obtained using a microscope slide scanner (PANNORAMIC MIDI II) in a bright field of view.

## RNA extraction and RT-qPCR

For RT-qPCR assays of various cell elongation- and lignification-related genes, the LM region in the leaf above the primary ear of different maize plants was collected for total RNA extraction. Total RNA extraction and RT-qPCR were performed as described previously. The primers used for RT-qPCR are listed in Supplemental Table 11.

## Plasmid construction

To generate the *35Sp:bHLH30-3FLAG* and *35Sp:bHLH155-3FLAG* constructs, the full-length coding regions of *bHLH30* and *bHLH155* were amplified from B73 and inserted into *Kpn*I- and *Sall*-digested *pPZP21-35Sp:3FLAG* (Ma et al., 2016). To generate the *PAL7p-G3:LUC*, *PAL7p-mG3:LUC*, *EXPA5p-E2:LUC*, and *EXPA5p-mE2:LUC* reporters, a set of 49-bp fragments containing either wild-type or mutated *cis*-elements from the *PAL7* or *EXPA5* promoter were inserted into the *Kpn*I-*Sall*-digested *pGreen-0800-35S* mini vector. The primers used for plasmid construction are listed in Supplemental Table 11.

## Maize protoplast transformation, ChIP, and transient expression assays

For maize protoplast transformation, protoplasts were isolated from the second leaves of 10-day-old etiolated seedlings of the B73 inbred line and transformed as described previously (Tu et al., 2020). The *35Sp:bHLH30-3FLAG* and *35Sp:bHLH155-3FLAG* plasmids were transformed into maize protoplasts, and the protoplasts were incubated under dim light conditions at 25°C. After 16–20 h of transformation, the protoplasts were harvested and used for ChIP assays, with anti-FLAG antibodies used for immunoprecipitation of *bHLH30-3FLAG* and *bHLH155-3FLAG* fusion proteins. For transient expression assays, the effectors *bHLH30-FLAG* and *bHLH155-FLAG* were co-expressed with the indicated *LUC* reporters in maize protoplasts following previously described procedures. The primers used for ChIP-qPCR are listed in Supplemental Table 11.

## Function of sclerenchyma cells in leaf angle regulation

### Statistical analysis

The data are presented as means ± SD ( $n \geq 3$ ). Different letters indicate statistically significant differences determined by ANOVA ( $p < 0.05$ ) for multiple comparisons, and values with the same letter are not significantly different.

## DATA AVAILABILITY

The raw bulk RNA-seq and snRNA-seq data from this study have been deposited at the China National Center for Bioinformation under accession number PRJCA020760. The gene sequence data can be found in MaizeGDB under the following accession numbers: *bHLH30* (Zm00001d018056), *bHLH155* (Zm00001d052254), *EXPA5* (Zm00001d038476), and *PAL7* (Zm00001d017279).

## SUPPLEMENTAL INFORMATION

Supplemental information is available at *Molecular Plant Online*.

## FUNDING

This work was supported by the National Natural Science Foundation of China (32270263), the Key R&D Program of Shandong Province (ZR202211070163), the Taishan Scholars program (to B.L.), and the China Postdoctoral Science Foundation (2023M742154).

## AUTHOR CONTRIBUTIONS

Q.W. performed the histological and molecular experiments. Q.G. and H.Y. performed the snRNA-seq library preparation and analysis. Q.S. and M.L. identified the mutants and conducted the phenotyping. Y.N. performed the RNA *in situ* hybridization assay. D.X., S.Q., and W.X. performed the histological analysis of various inbred lines. X.C. and L.L. conducted the bulk RNA-seq analysis. F.K. and H.Z. analyzed the data. P.L., B.L., and G.L. conceived the project and provided the materials. Q.W., B.L., and G.L. wrote the manuscript.

## ACKNOWLEDGMENTS

No conflict of interest is declared.

Received: November 16, 2023

Revised: April 17, 2024

Accepted: May 5, 2024

Published: May 7, 2024

## REFERENCES

- Assefa, Y., Carter, P., Hinds, M., Bhalla, G., Schon, R., Jeschke, M., Paszkiewicz, S., Smith, S., and Ciampitti, I.A. (2018). Analysis of Long Term Study Indicates Both Agronomic Optimal Plant Density and Increase Maize Yield per Plant Contributed to Yield Gain. Sci. Rep. **8**:4937. <https://doi.org/10.1038/s41598-018-23362-x>.
- Cao, Y., Zhong, Z., Wang, H., and Shen, R. (2022). Leaf angle: a target of genetic improvement in cereal crops tailored for high-density planting. Plant Biotechnol. J. **20**:426–436. <https://doi.org/10.1111/pbi.13780>.
- Cao, Y., Zeng, H., Ku, L., Ren, Z., Han, Y., Su, H., Dou, D., Liu, H., Dong, Y., Zhu, F., et al. (2020). ZmlBH1-1 regulates plant architecture in maize. J. Exp. Bot. **71**:2943–2955. <https://doi.org/10.1093/jxb/eraa052>.
- Chaffey, N. (2008). Physiological anatomy and function of the membranous grass ligule. New Phytol. **146**:5–21. <https://doi.org/10.1046/j.1469-8137.2000.00618.x>.
- Chaffey, N.J. (1994). Structure and function of the membranous grass ligule: a comparative study. Bot. J. Linn. Soc. **116**:53–69. <https://doi.org/10.1111/j.1095-8339.1994.tb00421.x>.
- Ding, J., Adiconis, X., Simmons, S.K., Kowalczyk, M.S., Hession, C.C., Marjanovic, N.D., Hughes, T.K., Wadsworth, M.H., Burks, T., Nguyen, L.T., et al. (2020). Systematic comparison of single-cell and

## Function of sclerenchyma cells in leaf angle regulation

## Molecular Plant

- single-nucleus RNA-sequencing methods. *Nat. Biotechnol.* **38**:737–746. <https://doi.org/10.1038/s41587-020-0465-8>.
- Dou, D., Han, S., Cao, L., Ku, L., Liu, H., Su, H., Ren, Z., Zhang, D., Zeng, H., Dong, Y., et al.** (2021). CLA4 regulates leaf angle through multiple hormone signaling pathways in maize. *J. Exp. Bot.* **72**:1782–1794. <https://doi.org/10.1093/jxb/eraa565>.
- Duan, H., Li, J., Sun, Y., Xiong, X., Sun, L., Li, W., Gao, J., Li, N., Zhang, J., Cui, J., et al.** (2022). Candidate loci for leaf angle in maize revealed by a combination of genome-wide association study and meta-analysis. *Front. Genet.* **13**:1004211. <https://doi.org/10.3389/fgene.2022.1004211>.
- Duvick, D.N.** (2005). Genetic progress in yield of United States maize (*Zea mays* L.). *Maydica* **50**:193–202.
- Dzievit, M.J., Li, X., and Yu, J.** (2019). Dissection of Leaf Angle Variation in Maize through Genetic Mapping and Meta-Analysis. *Plant Genome* **12**:12. <https://doi.org/10.3835/plantgenome2018.05.0024>.
- Han, X., Zhang, Y., Lou, Z., Li, J., Wang, Z., Gao, C., Liu, Y., Ren, Z., Liu, W., Li, B., et al.** (2023). Time series single-cell transcriptional atlases reveal cell fate differentiation driven by light in *Arabidopsis* seedlings. *Nat. Plants* **9**:2095–2109. <https://doi.org/10.1038/s41477-023-01544-4>.
- Ji, X., Gao, Q., Chen, F., Bai, M., Zhuang, Z., and Peng, Y.** (2022). Mutant Ipa1 Analysis of ZmLPA1 Gene Regulates Maize Leaf-Angle Development through the Auxin Pathway. *Int. J. Mol. Sci.* **23**. <https://doi.org/10.3390/ijms23094886>.
- Johnston, R., Wang, M., Sun, Q., Sylvester, A.W., Hake, S., and Scanlon, M.J.** (2014). Transcriptomic analyses indicate that maize ligule development recapitulates gene expression patterns that occur during lateral organ initiation. *Plant Cell* **26**:4718–4732. <https://doi.org/10.1105/tpc.114.132688>.
- Khaipho-Burch, M., Cooper, M., Crossa, J., de Leon, N., Holland, J., Lewis, R., McCouch, S., Murray, S.C., Rabbi, I., Ronald, P., et al.** (2023). Genetic modification can improve crop yields - but stop overselling it. *Nature* **621**:470–473. <https://doi.org/10.1038/d41586-023-02895-w>.
- Kong, F., Zhang, T., Liu, J., Heng, S., Shi, Q., Zhang, H., Wang, Z., Ge, L., Li, P., Lu, X., and Li, G.** (2017). Regulation of Leaf Angle by Auricle Development in Maize. *Mol. Plant* **10**:516–519. <https://doi.org/10.1016/j.molp.2017.02.001>.
- Ku, L.X., Zhang, J., Guo, S.L., Liu, H.Y., Zhao, R.F., and Chen, Y.H.** (2012). Integrated multiple population analysis of leaf architecture traits in maize (*Zea mays* L.). *J. Exp. Bot.* **63**:261–274. <https://doi.org/10.1093/jxb/err277>.
- Li, C., Li, Y., Song, G., Yang, D., Xia, Z., Sun, C., Zhao, Y., Hou, M., Zhang, M., Qi, Z., et al.** (2023). Gene expression and expression quantitative trait loci analyses uncover natural variations underlying the improvement of important agronomic traits during modern maize breeding. *Plant J.* **115**:772–787. <https://doi.org/10.1111/tpj.16260>.
- Li, H., Wang, L., Liu, M., Dong, Z., Li, Q., Fei, S., Xiang, H., Liu, B., and Jin, W.** (2020). Maize Plant Architecture Is Regulated by the Ethylene Biosynthetic Gene ZmACS7. *Plant Physiol.* **183**:1184–1199. <https://doi.org/10.1104/pp.19.01421>.
- Liu, F., Song, Q., Zhao, J., Mao, L., Bu, H., Hu, Y., and Zhu, X.G.** (2021a). Canopy occupation volume as an indicator of canopy photosynthetic capacity. *New Phytol.* **232**:941–956. <https://doi.org/10.1111/nph.17611>.
- Liu, G.Z., Yang, Y.S., Liu, W.M., Guo, X.X., Xie, R.Z., Ming, B., Xue, J., Zhang, G.Q., Li, R.F., Wang, K.R., et al.** (2022). Optimized Canopy Structure Improves Maize Grain Yield and Resource Use Efficiency11 (Food and Energy Security), p. e375, ARTN e375. <https://doi.org/10.1002/fes.375>.
- Liu, X., Bourgault, R., Galli, M., Strable, J., Chen, Z., Feng, F., Dong, J., Molina, I., and Gallavotti, A.** (2021b). The FUSED LEAVES1-
- ADHERENT1 regulatory module is required for maize cuticle development and organ separation. *New Phytol.* **229**:388–402. <https://doi.org/10.1111/nph.16837>.
- Ma, L., Tian, T., Lin, R., Deng, X.W., Wang, H., and Li, G.** (2016). Arabidopsis FHY3 and FAR1 Regulate Light-Induced myo-Inositol Biosynthesis and Oxidative Stress Responses by Transcriptional Activation of MIPS1. *Mol. Plant* **9**:541–557. <https://doi.org/10.1016/j.molp.2015.12.013>.
- Makarevitch, I., Thompson, A., Muehlbauer, G.J., and Springer, N.M.** (2012). Brd1 gene in maize encodes a brassinosteroid C-6 oxidase. *PLoS One* **7**:e30798. <https://doi.org/10.1371/journal.pone.0030798>.
- Mantilla-Perez, M.B., and Salas Fernandez, M.G.** (2017). Differential manipulation of leaf angle throughout the canopy: current status and prospects. *J. Exp. Bot.* **68**:5699–5717. <https://doi.org/10.1093/jxb/erx378>.
- Marand, A.P., Chen, Z., Gallavotti, A., and Schmitz, R.J.** (2021). A cis-regulatory atlas in maize at single-cell resolution. *Cell* **184**:3041–3055.e21. <https://doi.org/10.1016/j.cell.2021.04.014>.
- Meng, Q., Hou, P., Wu, L., Chen, X., Cui, Z., and Zhang, F.** (2013). Understanding production potentials and yield gaps in intensive maize production in China. *Field Crops Res.* **143**:91–97. <https://doi.org/10.1016/j.fcr.2012.09.023>.
- Moreno, M.A., Harper, L.C., Krueger, R.W., Dellaporta, S.L., and Freeling, M.** (1997). liguleless1 encodes a nuclear-localized protein required for induction of ligules and auricles during maize leaf organogenesis. *Genes Dev.* **11**:616–628. <https://doi.org/10.1101/gad.11.5.616>.
- Neher, W.R., Rasmussen, C.G., Braybrook, S.A., Lazetic, V., Stowers, C.E., Mooney, P.T., Sylvester, A.W., and Springer, P.S.** (2023). The maize preligule band is subdivided into distinct domains with contrasting cellular properties prior to ligule outgrowth. *Development*, 150. <https://doi.org/10.1242/dev.201608>.
- Peng, B., Zhao, X., Wang, Y., Li, C., Li, Y., Zhang, D., Shi, Y., Song, Y., Wang, L., Li, Y., and Wang, T.** (2021). Genome-wide association studies of leaf angle in maize. *Mol. Breed.* **41**:50. <https://doi.org/10.1007/s11032-021-01241-0>.
- Qin, X., Feng, F., Li, Y., Xu, S., Siddique, K.H.M., Liao, Y., and Lübbenstedt, T.** (2016). Maize yield improvements in China: past trends and future directions. *Plant Breed.* **135**:166–176. <https://doi.org/10.1111/pbr.12347>.
- Ren, Z., Wu, L., Ku, L., Wang, H., Zeng, H., Su, H., Wei, L., Dou, D., Liu, H., Cao, Y., et al.** (2020). ZmIL1 regulates leaf angle by directly affecting liguleless1 expression in maize. *Plant Biotechnol. J.* **18**:881–883. <https://doi.org/10.1111/pbi.13255>.
- Satterlee, J.W., Strable, J., and Scanlon, M.J.** (2020). Plant stem-cell organization and differentiation at single-cell resolution. *Proc. Natl. Acad. Sci. USA* **117**:33689–33699. <https://doi.org/10.1073/pnas.2018788117>.
- Shah, A.N., Tanveer, M., Abbas, A., Yildirim, M., Shah, A.A., Ahmad, M.I., Wang, Z., Sun, W., and Song, Y.** (2021). Combating Dual Challenges in Maize Under High Planting Density: Stem Lodging and Kernel Abortion. *Front. Plant Sci.* **12**:699085. <https://doi.org/10.3389/fpls.2021.699085>.
- Song, X., Guo, P., Xia, K., Wang, M., Liu, Y., Chen, L., Zhang, J., Xu, M., Liu, N., Yue, Z., et al.** (2023). Spatial transcriptomics reveals light-induced chlorenchyma cells involved in promoting shoot regeneration in tomato callus. *Proc. Natl. Acad. Sci. USA* **120**:e2310163120. <https://doi.org/10.1073/pnas.2310163120>.
- Strable, J., Wallace, J.G., Unger-Wallace, E., Briggs, S., Bradbury, P.J., Buckler, E.S., and Vollbrecht, E.** (2017). Maize YABBY Genes drooping leaf1 and drooping leaf2 Regulate Plant Architecture. *Plant Cell* **29**:1622–1641. <https://doi.org/10.1105/tpc.16.00477>.

## Molecular Plant

- Sun, G., Xia, M., Li, J., Ma, W., Li, Q., Xie, J., Bai, S., Fang, S., Sun, T., Feng, X., et al.** (2022). The maize single-nucleus transcriptome comprehensively describes signaling networks governing movement and development of grass stomata. *Plant Cell* **34**:1890–1911. <https://doi.org/10.1093/plcell/koac047>.
- Sylvester, A.W., Cande, W.Z., and Freeling, M.** (1990). Division and differentiation during normal and liguleless-1 maize leaf development. *Development* **110**:985–1000. <https://doi.org/10.1242/dev.110.3.985>.
- Tian, F., Bradbury, P.J., Brown, P.J., Hung, H., Sun, Q., Flint-Garcia, S., Rochefford, T.R., McMullen, M.D., Holland, J.B., and Buckler, E.S.** (2011). Genome-wide association study of leaf architecture in the maize nested association mapping population. *Nat. Genet.* **43**:159–162. <https://doi.org/10.1038/ng.746>.
- Tian, J., Wang, C., Xia, J., Wu, L., Xu, G., Wu, W., Li, D., Qin, W., Han, X., Chen, Q., et al.** (2019). Teosinte ligule allele narrows plant architecture and enhances high-density maize yields. *Science* **365**:658–664. <https://doi.org/10.1126/science.aax5482>.
- Tu, X., Mejía-Guerra, M.K., Valdes Franco, J.A., Tzeng, D., Chu, P.Y., Shen, W., Wei, Y., Dai, X., Li, P., Buckler, E.S., and Zhong, S.** (2020). Reconstructing the maize leaf regulatory network using ChIP-seq data of 104 transcription factors. *Nat. Commun.* **11**:5089. <https://doi.org/10.1038/s41467-020-18832-8>.
- Walsh, J., Waters, C.A., and Freeling, M.** (1998). The maize gene liguleless2 encodes a basic leucine zipper protein involved in the establishment of the leaf blade-sheath boundary. *Genes Dev.* **12**:208–218. <https://doi.org/10.1101/gad.12.2.208>.
- Wang, B., Lin, Z., Li, X., Zhao, Y., Zhao, B., Wu, G., Ma, X., Wang, H., Xie, Y., Li, Q., et al.** (2020a). Genome-wide selection and genetic improvement during modern maize breeding. *Nat. Genet.* **52**:565–571. <https://doi.org/10.1038/s41588-020-0616-3>.
- Function of sclerenchyma cells in leaf angle regulation**
- Wang, X., Wang, X., Sun, S., Tu, X., Lin, K., Qin, L., Wang, X., Li, G., Zhong, S., and Li, P.** (2022). Characterization of regulatory modules controlling leaf angle in maize. *Plant Physiol.* **190**:500–515. <https://doi.org/10.1093/plphys/kiac308>.
- Wang, X., Shi, Z., Zhang, R., Sun, X., Wang, J., Wang, S., Zhang, Y., Zhao, Y., Su, A., Li, C., et al.** (2020b). Stalk architecture, cell wall composition, and QTL underlying high stalk flexibility for improved lodging resistance in maize. *BMC Plant Biol.* **20**:515. <https://doi.org/10.1186/s12870-020-02728-2>.
- Xu, X., Crow, M., Rice, B.R., Li, F., Harris, B., Liu, L., Demesa-Arevalo, E., Lu, Z., Wang, L., Fox, N., et al.** (2021). Single-cell RNA sequencing of developing maize ears facilitates functional analysis and trait candidate gene discovery. *Dev. Cell* **56**:557–568.e6. <https://doi.org/10.1016/j.devcel.2020.12.015>.
- Zhang, L.Y., Bai, M.Y., Wu, J., Zhu, J.Y., Wang, H., Zhang, Z., Wang, W., Sun, Y., Zhao, J., Sun, X., et al.** (2009). Antagonistic HLH/bHLH transcription factors mediate brassinosteroid regulation of cell elongation and plant development in rice and *Arabidopsis*. *Plant Cell* **21**:3767–3780. <https://doi.org/10.1105/tpc.109.070441>.
- Zhao, S., Li, X., Song, J., Li, H., Zhao, X., Zhang, P., Li, Z., Tian, Z., Lv, M., Deng, C., et al.** (2022). Genetic dissection of maize plant architecture using a novel nested association mapping population. *Plant Genome* **15**:e20179. <https://doi.org/10.1002/tpg2.20179>.
- Zhou, L.J., Xiao, L.T., and Xue, H.W.** (2017). Dynamic Cytology and Transcriptional Regulation of Rice Lamina Joint Development. *Plant Physiol.* **174**:1728–1746. <https://doi.org/10.1104/pp.17.00413>.
- Zhu, Y., Song, B., Guo, Y., Wang, B., Xu, C., Zhu, H., E, L., Lai, J., Song, W., and Zhao, H.** (2023). QTL Analysis Reveals Conserved and Differential Genetic Regulation of Maize Lateral Angles above the Ear. *Plants*, **12**. <https://doi.org/10.3390/plants12030680>.